Outage of Cognitive Electric Vehicle Networks Over Mixed RF/VLC Channels With Signal-Dependent Noise and Imperfect CSI

Galymzhan Nauryzbayev, *Member, IEEE*, Mohamed Abdallah, *Senior Member, IEEE*, Imran S. Ansari, *Member, IEEE*, Naofal Al-Dhahir, *Fellow, IEEE*, and Khalid Qaraqe, *Senior Member, IEEE*

***Abstract*—In this paper, we propose a novel jamming-robust communication technique for the outdoor cognitive EV-enabled network over mixed radio-frequency (RF)/visible light communication (VLC) channels with signal-dependent noise. One EV acts as a relaying node to allow an aggregator to reach the jammed EV and, at the same time, operates in both RF and VLC spectrum bands while satisfying interference constraints imposed by the primary network entities. We derive an exact closed-form analytical expression for the outage probability and also provide its asymptotic analysis while considering various channel state information quality scenarios. Finally, simulation results validate the accuracy of our analysis.**

***Index Terms*—Cognitive radio (CR), electrical vehicle (EV), outage probability (OP), visible light communication (VLC).**

I. Introduction

THE modern transportation infrastructure is noted to be a source of the harmful carbon dioxide (CO_2) emissions that increase the global temperature, e.g., in the United States it was responsible for 27% of the entire greenhouse impact [1]. This dire situation can be mitigated to a great extent by enabling massive use of electrical vehicles (EVs) known for being highly efficient power grid (PG) cells with lower CO_2 emission. This PG-EV integration can only be attained by deploying reliable and secure communication systems that, in turn, impose vulnerabilities to their typical cyber security threats [2]–[4]. For instance, an illegitimate user can distort or jam the radio frequency (RF) signal by making it unrecognizable at the critical PG nodes and disable the operation of a large area through local load unbalancing [3]. To overcome this issue, visible light communications (VLC) has been recognized as an alternative solution due to its electromagnetic immunity to the RF interference for possible applications in indoor and outdoor environments, e.g., intelligent transportation systems (ITSs) [5]–[7]. For instance, the authors in [5] studied the use of smart automotive lighting designed for the ITSs by combining the visible light positioning and VLC. In [6], a vehicle-to-vehicle VLC system was designed and implemented. In [7], an analytical line-of-sight (LOS) path-loss model was proposed for the outdoor VLC ITSs. However, the channel models in [5]–[7] only considered the Lambertian-emission based path-loss and the considered noise terms were all assumed to be additive white Gaussian distributed and independent of the signal. These noise models neglect a fundamental issue: the noise in the outdoor scenario depends on the signal itself due to the random nature of photon emission in the laser diode affected by the atmosphere turbulence (which degrades the link performance) [8].

Hybrid RF/VLC systems are well analyzed in the open literature as a productive solution to various issues that pertain to both these technologies, i.e., RF and VLC, [9], [10] and references therein. For instance, [9] designs a hybrid system with multiple VLC and RF links demonstrating the combined benefits of both technologies, i.e., high data rate offered by VLC and ubiquitous coverage offered by RF. Similarly, [10] investigates cooperative load balancing under hybrid RF/VLC systems and demonstrates that the performance, in terms of throughput and fairness, is highest for the hybrid RF/VLC systems, amongst the considered scenarios therein.

In contrast to these studies, in this paper, we consider the presence of the signal-dependent noise (SDN) term caused by the random nature of photon emissions in the diode [11]. Subsequently, we investigate the outage performance of the downlink outdoor vehicular network with two EVs with an enabled cognitive radio (CR) capability to avoid severe interference in the primary network (PN) by setting an interference temperature constraint (ITC). We summarize our contributions as follows. Firstly, we derive a new closed-form expression for the effective outage probability (OP) of the outdoor CR relaying network over mixed RF-RF/VLC channels for various channel state information (CSI) scenarios. Second, we provide an asymptotic analysis for the OP. Finally, the provided analysis is validated by Monte Carlo simulations.

II. System Model

The adopted system model represents a downlink outdoor network with an aggregator (A), two EVs (D_1 and D_2) and a jamming (J) node. The PN communication session takes place between the aggregator and EVs while the secondary network (SN) includes only communication between the EVs. Moreover, it is assumed that the A-to-D_1 communication link is jammed and, then, D_2 acts as a relay (in the decode-and-forward (DF) mode [12], [13]) to forward the desired data to the jammed EV. The end-to-end communication is realized over two identical time slots, with duration of $T/2$ each, where T stands for the time period over which the channel estimates are assumed to remain constant. In the PN, communication is organized in the RF spectrum due to its wide coverage and non-line-of-sight (NLOS) nature while, in the SN, the EVs can communicate with each other through the RF or VLC channels. In order to support the PN communication, the RF link between the EVs adopts the CR approach to guarantee a tolerable ITC level, denoted by I_{PU}, at the primary user (PU). For practical reasons, the RF links are modeled as $h_i = \tilde{h}_i + \epsilon$, $\forall \in \mathcal{A} = \{1, 2, 3\}$, where $\tilde{h}_i$ and ϵ denote the channel estimate and the estimation error, with $\mathcal{CN}(0, \sigma_\epsilon^2)$, respectively [14].

The received signal at the relay (i.e., D_2) can be written as

$$y_r^{\mathrm{RF}} = \sqrt{P_s d_1^{-\tau}} h_1 s + n_r$$

Manuscript received April 29, 2019; revised December 21, 2019; accepted March 5, 2020. Date of publication April 20, 2020; date of current version June 18, 2020. This work was supported by the Nazarbayev University Faculty Development Competitive Research Program under Grant 240919FD3935 (SEDS2020014). The review of this article was coordinated by Dr. X. Dong. *(Corresponding author: Galymzhan Nauryzbayev.)*

Galymzhan Nauryzbayev is with the Department of Electrical and Computer Engineering (ECE), School of Engineering and Digital Sciences, Nazarbayev University, Nur-Sultan City 010000, Kazakhstan (e-mail: galymzhan.nauryzbayev@nu.edu.kz).

Mohamed Abdallah is with the Division of Information and Computing Technology, College of Science and Engineering, Hamad Bin Khalifa University, Qatar Foundation, Doha, Qatar (e-mail: moabdallah@hbku.edu.qa).

Imran S. Ansari is with the School of Engineering, University of Glasgow, Glasgow G12 8QQ, U.K. (e-mail: ansarimran@ieee.org).

Naofal Al-Dhahir is with the Department of ECE, University of Texas at Dallas, Dallas, TX 75080 USA (e-mail: aldhahir@utdallas.edu).

Khalid Qaraqe is with the Department of ECE, Texas A&M University at Qatar, Doha, Qatar (e-mail: khalid.qaraqe@qatar.tamu.edu).

Digital Object Identifier 10.1109/TVT.2020.2981871

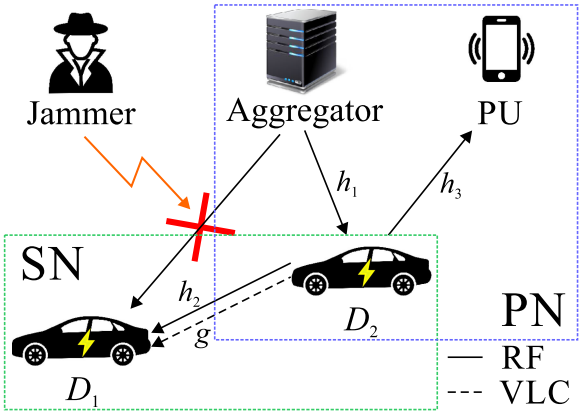

Fig. 1. System model of the outdoor CR-based EV network.

$$= \sqrt{P_s d_1^{-\tau}} \tilde{h}_1 s + \sqrt{P_s d_1^{-\tau}} \epsilon s + n_r, \tag{1}$$

where P_s, s, h_1, d_1, τ, and n_r denote the source transmit power, the transmit signal, the channel coefficient between A and D_2, the corresponding distance, the path-loss exponent, and the additive white Gaussian noise (AWGN) term, with zero-mean and variance σ_r^2, respectively. Therefore, the corresponding signal-to-interference-plus-noise ratio (SINR) at D_2 can be expressed as

$$\gamma_r^{\mathrm{RF}} = \frac{P_s |\tilde{h}_1|^2}{P_s \sigma_\epsilon^2 + d_1^\tau \sigma_r^2}. \tag{2}$$

It is reasonable to assume that D_1 can acquire the RF- and VLC-based CSI estimates between D_2 and itself, and then feed them back to the relay which, in turn, decodes and forward the received message via the best channel. Thus, the received signal at the destination (i.e., D_1) over the RF channel can be formulated as

$$\begin{aligned} y_d^{\mathrm{RF}} &= \sqrt{P_r d_2^{-\tau}} h_2 s + n_d \\ &= \sqrt{P_r d_2^{-\tau}} \tilde{h}_2 s + \sqrt{P_r d_2^{-\tau}} \epsilon s + n_d, \end{aligned} \tag{3}$$

where P_r, h_2, d_2 and n_d denote the relay transmit power, the channel coefficient between D_2 and D_1, the corresponding distance, and the AWGN noise, with variance σ_d^2, respectively. Hence, we can write the corresponding SINR at D_1 as

$$\gamma_d^{\mathrm{RF}} = \frac{P_r |\tilde{h}_2|^2}{P_r \sigma_\epsilon^2 + d_2^\tau \sigma_d^2}. \tag{4}$$

Moreover, the relay transmit power is constrained as $P_r = \min(\frac{I_{PU} d_3^\tau}{|h_3|^2}, \bar{P}_r)$, where $\bar{P}_r$ is the maximum available relay transmit power and h_3 denotes the channel coefficient between D_2 and PU, with a respective distance d_3.

Regarding the VLC link, we consider an outdoor vehicular VLC (V2LC) scenario, where a point-to-point communication link is established between the headlight (a light-emitting diode (LED) is used as the transmitter) of D_2 and the tail (a positive-intrinsic-negative photodetector (PIN PD) is installed as the receiver) of D_1. In [15], the authors experimentally verified that the outdoor V2LC links experience the Rician fading in addition to the Lambertian-emission based path-loss. Hence, the received signal is given as [11]

$$\begin{aligned} y_d^{\mathrm{VLC}} &= \rho g x + \sqrt{\rho g x} n_D + n_I \\ &= \rho g_L g_R x + \sqrt{\rho g_L g_R x} n_D + n_I \\ &= \rho g_L \left(\tilde{g}_R + \epsilon_R\right) x + \sqrt{\rho g_L \left(\tilde{g}_R + \epsilon_R\right) x} n_D + n_I \\ &= \rho g_L \tilde{g}_R x + \rho g_L \epsilon_R x \\ &\quad + \sqrt{\rho g_L \left(\tilde{g}_R + \epsilon_R\right) x} n_D + n_I, \end{aligned} \tag{5}$$

where $g = g_L g_R$ denotes the composite VLC channel gain in the outdoor environment [16]. g_L is the path-loss following Lambertian emission, ρ denotes the effective photo-current conversion ratio, and $g_R = \tilde{g}_R + \epsilon_R$ is the atmospheric turbulence, where $\tilde{g}_R$ and ϵ_R denote the estimated atmospheric turbulence and corresponding estimation error, with variance $\sigma_{\epsilon_R}^2$, respectively. x is the transmit signal, with $\mathbb{E}\{x\} = P_t$, where P_t denotes the average optical intensity. n_D and n_I are the mutually independent signal-dependent and signal-independent Gaussian random variables (RVs), with variances $\xi^2 \sigma_D^2$ and σ_I^2, respectively. Therefore, the corresponding SINR is given by [17]

$$\gamma_d^{\mathrm{VLC}} = \frac{(\rho g_L \tilde{g}_R P_t)^2}{(\rho g_L P_t)^2 \sigma_{\epsilon_R}^2 + \rho g_L \left(\tilde{g}_R + \sigma_{\epsilon_R}\right) P_t \xi^2 \sigma_D^2 + \sigma_I^2}, \tag{6}$$

where P_t and $\xi^2 > 0$ are the message power and the SDN factor, respectively. g_L is modeled as [18]

$$g_L = \begin{cases} \frac{(m+1) A_r}{2\pi d^2} \frac{\cos^m(\phi) \cos(\psi)}{(T_s(\psi) g(\psi))^{-1}}, & \text{if } 0 \le \psi \le \Psi, \\ 0, & \text{if } \psi > \Psi, \end{cases} \tag{7}$$

where d is the distance, ϕ is the angle of irradiance, ψ is the angle of incidence, $T_s(\psi)$ is the optical filter gain, $g(\psi)$ is the concentrator gain, A_r is the area of PIN PD, and Ψ is the field-of-view (FOV). The Lambertian radiation pattern order is determined by $m = -(\log_2(\cos(\Phi_{1/2})))^{-1}$, where $\Phi_{1/2}$ is the LED semi-angle (at half power).

The noise variance σ_I^2 of the PIN PD is the summation of the variances of the shot and thermal noises given as

$$\sigma_{shot}^2 = 2q\rho I_{bg} I_2 R_b, \tag{8}$$

$$\sigma_{thermal}^2 = \frac{8\pi k T_k \eta A_r I_2 R_b^2}{G} + \frac{16\pi^2 k T_k \Gamma \eta^2 A^2 I_3 R_b^3}{g_m}, \tag{9}$$

where q is the electronic charge constant, I_{bg} is the background current, I_2 and I_3 are the noise bandwidth factors, R_b is the data rate, k is the Boltzmann's constant, T_k is the absolute temperature, η is the fixed capacitance, Γ is the field effect transistor (FET) channel noise factor, G is the gain of open-loop voltage, and g_m is the FET transconductance.

III. Performance Analysis

Assuming that the DF relaying mode is employed and the best channel is selected for the D_2-to-D_1 transmission, the effective signal-to-noise ratio (SNR) can be expressed as

$$\gamma^{\mathrm{DF}} = \min\left(\gamma_r, \gamma_d\right), \tag{10}$$

where $\gamma_d = \max(\gamma_d^{\mathrm{RF}}, \gamma_d^{\mathrm{VLC}})$. Hence, the OP is defined as

$$\begin{aligned} P_{\mathrm{out}} &= \Pr\left(\min\left(\gamma_r, \gamma_d\right) < v\right) \\ &= 1 - \Pr\left(\min\left(\gamma_r, \gamma_d\right) > v\right) \\ &= 1 - \underbrace{\Pr\left(\gamma_r > v\right)}_{B} \underbrace{\Pr\left(\gamma_d > v\right)}_{C}, \end{aligned} \tag{11}$$

where $v = 2^{2\mathcal{R}} - 1$ denotes the SNR-based data rate threshold, where $\mathcal{R}$ is the rate threshold.

The term B can be calculated using Eq. (2) as

$$B = 1 - \Pr\left(|\tilde{h}_1|^2 < \frac{v\left(P_s\sigma_\epsilon^2 + d_1^\tau\sigma_r^2\right)}{P_s}\right) = \exp\left(-\tilde{\lambda}_1 v\sigma_\epsilon^2\right)\exp\left(-\frac{\tilde{\lambda}_1 v d_1^\tau\sigma_r^2}{P_s}\right). \quad (12)$$

Note that $|h_i|^2, \forall i \in \mathcal{A}$, follows an exponential probability distribution [14], and $\tilde{\lambda}_1$ is the rate parameter of the RV $|\tilde{h}_1|^2$.

Next, the term C is given by

$$C = \Pr\left(\max\left(\gamma_d^{\mathrm{RF}}, \gamma_d^{\mathrm{VLC}}\right) > v\right) = 1 - \underbrace{\Pr\left(\gamma_d^{\mathrm{RF}} < v\right)}_{C_1}\underbrace{\Pr\left(\gamma_d^{\mathrm{VLC}} < v\right)}_{C_2}. \quad (13)$$

Considering the ITC, the cumulative density function (CDF) C_1 of γ_d^{RF} can be computed as

$$C_1 = \Pr\left(\gamma_d^{\mathrm{RF}} < v\right) = C_{11} + C_{12}, \quad (14)$$

where, due to the independence of the RVs in C_{11}, we have

$$C_{11} = \Pr\left(|\tilde{h}_2|^2 < \frac{v\left(\bar{P}_r\sigma_\epsilon^2 + d_2^\tau\sigma_d^2\right)}{\bar{P}_r}, |h_3|^2 < \frac{I_{PU}d_3^\tau}{\bar{P}_r}\right) = \left[1 - \exp\left(-\tilde{\lambda}_2 v\sigma_\epsilon^2\right)\exp\left(-\frac{\tilde{\lambda}_2 v d_2^\tau\sigma_d^2}{\bar{P}_r}\right)\right] \times \left[1 - \exp\left(-\frac{I_{PU}d_3^\tau}{\bar{P}_r}\right)\right], \quad (15)$$

and C_{12} is computed, after some algebraic manipulations, as

$$C_{12} = \Pr\left(|\tilde{h}_2|^2 < v\sigma_\epsilon^2 + \frac{v d_2^\tau\sigma_d^2|h_3|^2}{I_{PU}d_3^\tau}, |h_3|^2 > \frac{I_{PU}d_3^\tau}{\bar{P}_r}\right) = \exp\left(-\frac{I_{PU}d_3^\tau}{\bar{P}_r}\right)\left[1 - \exp\left(-\tilde{\lambda}_2 v\sigma_\epsilon^2\right) \times \left(1 + \frac{\tilde{\lambda}_2 v d_2^\tau\sigma_d^2}{I_{PU}d_3^\tau}\right)^{-1}\exp\left(-\frac{\tilde{\lambda}_2 v d_2^\tau\sigma_d^2}{\bar{P}_r}\right)\right]. \quad (16)$$

Hence, the CDF of γ_d^{RF} can be expressed as

$$C_1 = 1 - \exp\left(-\tilde{\lambda}_2 v\sigma_\epsilon^2\right)\exp\left(-\frac{\tilde{\lambda}_2 v d_2^\tau\sigma_d^2}{\bar{P}_r}\right) \times \left[1 - (1 - \Sigma)\exp\left(-\frac{I_{PU}d_3^\tau}{\bar{P}_r}\right)\right], \quad (17)$$

where $\Sigma = (1 + \frac{\tilde{\lambda}_2 v d_2^\tau\sigma_d^2}{I_{PU}d_3^\tau})^{-1}$ represents the impact of CR communication. Next, using Eq. (6), we rewrite the term C_2, i.e., the CDF of γ_d^{VLC} involving the SDN, as

$$C_2 = \Pr\left(\gamma_d^{\mathrm{VLC}} < v\right) = \Pr\left(\frac{(\rho g_L\tilde{g}_R P_t)^2}{(\rho g_L P_t)^2\sigma_{\epsilon_R}^2 + \rho g_L\left(\tilde{g}_R + \sigma_{\epsilon_R}\right)P_t\xi^2\sigma_D^2 + \sigma_I^2} < v\right) = \Pr\left((\rho g_L\tilde{g}_R P_t)^2 - v\rho g_L\tilde{g}_R P_t\xi^2\sigma_D^2 < v\left[(\rho g_L P_t)^2\sigma_{\epsilon_R}^2 + \rho g_L\sigma_{\epsilon_R}P_t\xi^2\sigma_D^2 + \sigma_I^2\right]\right). \quad (18)$$

Since $\tilde{g}_R$ follows the Rician distribution [15], the corresponding probability density function (PDF) is given by [19]

$$f_X(x) = \frac{x}{N}\exp\left(-\frac{x^2 + s^2}{2N}\right)I_0\left(\frac{xs}{N}\right), \quad (19)$$

where I_0 denotes the modified first kind Bessel function of order zero while s and N stand for the characteristic parameters of the Rician distribution.[1] After some algebraic manipulations, the CDF of γ_d^{VLC} can be found as in Eq. (20) shown at the bottom of this page, where Q_1 is the Marcum Q-function of order 1. Then, substituting C_1 and C_2, the term C can be expressed as shown in Eq. (21) at the bottom of this page. Finally, substituting B and C into Eq. (11), the OP can be given in closed form as in Eq. (22) shown at the bottom of this page.

[1]Moreover, we define another parameter, known as a shape parameter $K = \frac{s^2}{2N}$, which represents the ratio of the power arrived from the LOS path to the power corresponding to the remaining NLOS component.

$$C_2 = 1 - Q_1\left(\frac{s}{\sqrt{N}}, \frac{\sqrt{v\left[(\rho g_L\sigma_{\epsilon_R}P_t)^2 + \rho g_L\sigma_{\epsilon_R}P_t\xi^2\sigma_D^2 + \sigma_I^2\right] + \left(\frac{1}{2}v\xi^2\sigma_D^2\right)^2} + \frac{1}{2}v\xi^2\sigma_D^2}}{\sqrt{N}\rho g_L P_t}\right) \quad (20)$$

$$C = 1 - \left[1 - \exp\left(-\tilde{\lambda}_2 v\sigma_\epsilon^2\right)\exp\left(-\frac{\tilde{\lambda}_2 v d_2^\tau\sigma_d^2}{\bar{P}_r}\right)\left(1 - (1 - \Sigma)\exp\left(-\frac{I_{PU}d_3^\tau}{\bar{P}_r}\right)\right)\right] \times \left[1 - Q_1\left(\frac{s}{\sqrt{N}}, \frac{\sqrt{v\left[(\rho g_L\sigma_{\epsilon_R}P_t)^2 + \rho g_L\sigma_{\epsilon_R}P_t\xi^2\sigma_D^2 + \sigma_I^2\right] + \left(\frac{1}{2}v\xi^2\sigma_D^2\right)^2} + \frac{1}{2}v\xi^2\sigma_D^2}}{\sqrt{N}\rho g_L P_t}\right)\right] \quad (21)$$

$$P_{\mathrm{out}}(v) = 1 - \exp\left(-\frac{\tilde{\lambda}_1 v d_1^\tau\sigma_r^2}{P_s}\right)\left[1 - \left[1 - \exp\left(-\tilde{\lambda}_2 v\sigma_\epsilon^2\right)\exp\left(-\frac{\tilde{\lambda}_2 v d_2^\tau\sigma_d^2}{\bar{P}_r}\right)\left(1 - (1 - \Sigma)\exp\left(-\frac{I_{PU}d_3^\tau}{\bar{P}_r}\right)\right)\right] \times \left[1 - Q_1\left(\frac{s}{\sqrt{N}}, \frac{\sqrt{v\left[(\rho g_L\sigma_{\epsilon_R}P_t)^2 + \rho g_L\sigma_{\epsilon_R}P_t\xi^2\sigma_D^2 + \sigma_I^2\right] + \left(\frac{1}{2}v\xi^2\sigma_D^2\right)^2} + \frac{1}{2}v\xi^2\sigma_D^2}}{\sqrt{N}\rho g_L P_t}\right)\right]\right]\exp\left(-\tilde{\lambda}_1 v\sigma_\epsilon^2\right) \quad (22)$$

TABLE I
SIMULATION PARAMETERS

Parameter	Value	Parameter	Value	Parameter	Value
The aggregator - EV 2 distance, d_1	10 m	Path-loss exponent, τ	3	Data rate, R_b	200 Mbits/s
The EV 1 - EV 2 distance, d_2	4 m	LED semi-angle, $\Phi_{1/2}$	60°	PIN PD FOV, Ψ_{FOV}	60°
The EV 2 - PU distance, d_3	10 m	Optical filter gain, $T(\psi_k)$	1	PIN PD detection area, A_r	10^{-4} m^2
Shape index (Rician fading), K	0 dB	Lambertian order, m	1	Background current, I_{bg}	10^3 μA
Photo-current conversion ratio, ρ	0.53 A/W	Noise bandwidth factor, I_2	0.562	Noise bandwidth factor, I_3	0.0868
Optical concentrator gain, $g(\psi_k)$	1	Absolute temperature, T_K	300 K	Open-loop voltage gain, G	10
Fixed capacitance, η	1.12 μF	FET channel noise factor, Γ	1.5	FET transconductance, g_m	30 mS

A. Asymptotic Analysis

To obtain meaningful insights on the impact of the involved fading parameters on the network performance, we investigate the system performance in the high SNR regime. By setting $\{P_s, P_r, P_t\} \to \infty$, the high SNR approximation of the end-to-end OP can be expressed as

$$P_{\text{out}}^{\text{asymp}-\text{RF/VLC}}(v) = 1 - \exp\left(-\tilde{\lambda}_1 v\sigma_\epsilon^2\right) \times \left[Q_1\left(\frac{s}{\sqrt{N}}, \sqrt{\frac{v\sigma_{\epsilon_R}^2}{N}}\right) + \exp\left(-\tilde{\lambda}_2 v\sigma_\epsilon^2\right)\left(1 - (1-\Sigma)\right.\right. \times \exp\left.\left.\left(-\frac{I_{PU} d_3^\tau}{\bar{P}_r}\right)\right)\left(1 - Q_1\left(\frac{s}{\sqrt{N}}, \sqrt{\frac{v\sigma_{\epsilon_R}^2}{N}}\right)\right)\right] \quad (23)$$

$$\underset{I_{PU}\to\infty}{\overset{(a)}{=}} 1 - \exp\left(-\tilde{\lambda}_1 v\sigma_\epsilon^2\right)\left[Q_1\left(\frac{s}{\sqrt{N}}, \sqrt{\frac{v\sigma_{\epsilon_R}^2}{N}}\right) + \exp\left(-\tilde{\lambda}_2 v\sigma_\epsilon^2\right)\left(1 - Q_1\left(\frac{s}{\sqrt{N}}, \sqrt{\frac{v\sigma_{\epsilon_R}^2}{N}}\right)\right)\right]. \quad (24)$$

Moreover, the (a) expression given by Eq. (24) represents the case when the relay transmit power P_r is not constrained, i.e., the secondary communication does not harm the primary receiver ($I_{PU} \to \infty$). As it can be seen from the general expression of the approximated OP, it depends on the quality of the CSI estimates and the maximum level of interference that PU can tolerate. Finally, in the case of perfect CSI, network failure will not occur, i.e., $P_{\text{out}}^{\text{asymp}-\text{RF/VLC}} = 0$ since $Q_1(a, 0) = 1$ for any a due to $\int_0^\infty f(x)\mathrm{d}x = 1$.

IV. DISCUSSION

In this section, we present numerical results on the outage performance of the outdoor cognitive EV network. The simulation parameters are presented in Table I. Without loss of generality, it is reasonable to assume that the LED and PIN PD comprising the secondary VLC communication link are aligned along a line perpendicular to the LED and PIN PD planes. Otherwise, the VLC channel gain will be decreased. Therefore, for simulation purposes, we assume $d_2 = 4$ m, with the corresponding VLC channel gain of -57 dB (calculated with respect to the simulation parameters[2] given in Table I). We also assume that, in the case of the RF channel, the source and relay transmit power levels are the same, i.e., $P = P_s = P_r$.

[2]Note that the simulation parameters are similar to [15]–[17], [20].

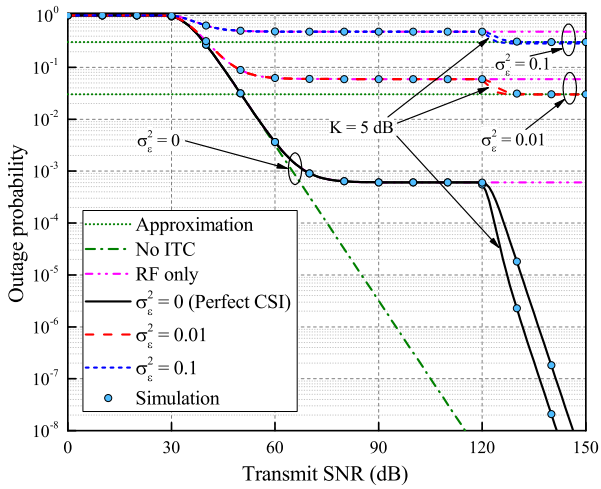

Fig. 2. The OP versus the transmit SNR for $g_L = 57$ dB, $v = 3$ dB, $I_{PU} = 25$ dB, $\xi^2 = 10$, and $K = \{0; 5\}$ dB.

In Fig. 2, we present some analytical and simulation results on the outage performance of the system under consideration. We evaluate the OP metric versus the transmit SNR which is defined as $\omega^{\text{Rayl}} = P/\sigma^2$ and $\omega^{\text{Rice}} = P_t/\sigma_I^2$ (for simplicity, we assume the same transmit SNR values for both RF and VLC communication links, i.e., $\omega = \omega^{\text{Rayl}} = \omega^{\text{Rice}}$).[3] From Fig. 2, we observe that the OP curves for the perfect CSI scenario outperform the other CSI scenarios, as expected. Moreover, we can see that the OP curves saturate due to the CR nature of transmission and then, after 120 dB, start improving. This can be explained by the fact that, within this saturation region, the RF-based SNR dominates the VLC-based one and the transmit power gets restricted to prevent harmful interference at PU. For instance, in the case when the RF links are deployed only, the announced ITC does not enable the OP curves' (plotted using Eq. (25) shown at the bottom of this page) enhancement, even in the high SNR region. However, in the high transmit SNR regime, the situation changes when the VLC-based SNR starts prevailing over the RF-based SNR. Moreover, since the VLC communication link does not interfere with the primary network, the OP performance starts improving by approaching the ideal case under the assumption that there is no ITC declared in the network. The ideal case without the CR-based saturation can be obtained by setting $\Sigma = 1$.

[3]With our assumptions and system parameters, it is reasonable to consider such high SNR values, e.g., 150 dB, which can be easily obtained due to the corresponding small variances of the noise terms.

$$P_{\text{out}}^{\text{RF/RF}}(v) = 1 - \exp\left(-\tilde{\lambda}_1 v\left(\sigma_\epsilon^2 + \frac{d_1^\tau \sigma_r^2}{P_s}\right)\right)\exp\left(-\tilde{\lambda}_2 v\left(\sigma_\epsilon^2 + \frac{d_2^\tau \sigma_d^2}{\bar{P}_r}\right)\right)\left(1 - (1-\Sigma)\exp\left(-\frac{I_{PU} d_3^\tau}{\bar{P}_r}\right)\right) \quad (25)$$

Moreover, it is worth pointing out that the curves related to the imperfect CSI scenarios ($\sigma_\epsilon^2 = 0.01$ and $\sigma_\epsilon^2 = 0.1$) follow the same behavior as the perfect CSI scenario, i.e., both saturation and further performance enhancement occur. However, they do not approach the ideal case and experience another saturation which is now caused by the CSI errors. These saturation curves coincide with the high SNR approximations of the OP performance given by Eq. (23). Finally, one can observe that the outage improves as the parameter K increases. This can be explained by the fact that more power (coming from the LOS path) consequently increases the effective VLC-based SINR. However, for imperfect CSI, the OP improvement is limited by the quality of CSI estimates. Another useful observation is that this improvement occurs exactly at the same transmit SNR value of approximately 120 dB and can be characterized by a steeper slope than the curve for $K = 0$ dB.

V. Conclusion

In this paper, we investigated the performance of the outdoor cognitive DF-based EV relaying network over mixed RF/VLC channels with the signal-dependent noise for different CSI scenarios. We derived a novel closed-form expression for the outage performance and analyzed its asymptotic behavior. We showed that the CSI quality dominates over the effect of power arrived from the LOS path. Finally, we demonstrated that the derived analytical results are in agreement with the Monte Carlo simulations.

References

[1] U.S. Environment Protection Agency, Sep. 2010, [Online]. Available: http://www.epa.gov/otaq/climate/basicinfo.htm#2

[2] T. Markel, M. Kuss and P. Denholm, "Communication and control of electric vehicles supporting renewables," in *Proc. IEEE Veh. Power Propulsion Syst. Conf.*, 2009, pp. 1–8.

[3] H. Su, M. Qiu and H. Wang, "Secure wireless communication system for smart grid with rechargeable electric vehicles," *IEEE Commun. Mag.*, vol. 50, no. 8, pp. 62–68, Aug. 2012.

[4] Y. Zhang, S. Gjessing, H. Liu, H. Ning, L. T. Yang and M. Guizani, "Securing vehicle-to-grid communications in the smart grid," *IEEE Wireless Commun.*, vol. 20, no. 6, pp. 66–73, Dec. 2013.

[5] S.-H. Yu, O. Shih, H. Tsai, N. Wisitpongphan and R. D. Roberts, "Smart automotive lighting for vehicle safety," *IEEE Commun. Mag.*, vol. 51, no. 12, pp. 50–59, Dec. 2013.

[6] N. A. Abdulsalam, R. A. Hajri, Z. A. Abri, Z. A. Lawati and M. M. Bait-Suwailam, "Design and implementation of a vehicle to vehicle communication system using Li-Fi technology," in *Proc. Int. Conf. Inf. Commun. Technol. Res.*, 2015, pp. 136–139.

[7] K. Cui *et al.*, "Traffic light to vehicle visible light communication channel characterization," *Appl. Opt.*, vol. 51, no. 27, pp. 6594–6605, Sep. 2012.

[8] J.-Y. Wang *et al.*, "Improvement of BER performance by tilting receiver plane for indoor visible light communications with input-dependent noise," in *Proc. IEEE Int. Conf. Commun.*, 2017, pp. 1–6.

[9] D. A. Basnayaka and H. Haas, "Design and analysis of a hybrid radio frequency and visible light communication system," *IEEE Trans. Commun.*, vol. 65, no. 10, pp. 4334–4347, Oct. 2017.

[10] X. Li, R. Zhang, and L. Hanzo, "Cooperative load balancing in hybrid visible light communications and WiFi," *IEEE Trans. Commun.*, vol. 63, no. 4, pp. 1319–1329, Apr. 2015.

[11] M. N. Khan and W. G. Cowley, "Signal dependent Gaussian noise model for FSO communications," *Australian Commun. Theory Workshop*, 2011, pp. 142–147.

[12] G. Nauryzbayev, M. Abdallah, and K. M. Rabie, "Outage probability of the EH-based full-duplex AF and DF relaying systems in α–μ environment," in *Proc. IEEE 88th Veh. Technol. Conf.*, 2018, pp. 1–6.

[13] S. Arzykulov, G. Nauryzbayev, T. A. Tsiftsis and B. Maham, "Performance analysis of underlay cognitive radio non-orthogonal multiple access networks," *IEEE Trans. Veh. Technol.*, vol. 68, no. 9, pp. 9318–9322, Sep. 2019.

[14] S. Arzykulov, T. A. Tsiftsis, G. Nauryzbayev and M. Abdallah, "Outage Performance of Cooperative Underlay CR-NOMA with Imperfect CSI," *IEEE Commun. Lett.*, vol. 23, no. 1, pp. 176–179, Jan. 2019.

[15] C. Li *et al.*, "Performance analysis of visible light communication using STBC-OFDM technique for intelligent transportation systems," *Int. J. Electron.*, vol. 101, no. 8, pp. 1117–1133, Aug. 2014.

[16] J. Wang *et al.*, "On the BER performance of relay-aided free-space optical communications in the presence of input-dependent noise," in *Proc. 9th Int. Conf. Wireless Commun. Signal Process.*, 2017, pp. 1–6.

[17] S. Lin *et al.*, "Outage performance analysis for outdoor vehicular visible light communications," in *Proc. 9th Int. Conf. Wireless Commun. Signal Process.*, 2017, pp. 1–5.

[18] G. Nauryzbayev, M. Abdallah and H. Elgala, "Outage of SEE-OFDM VLC-NOMA networks," *IEEE Photon. Technol. Lett.*, vol. 31, no. 2, pp. 121–124, Jan. 2019.

[19] H. Yang and M.-S. Alouini, *Order Statistics in Wireless Communications: Diversity, Adaptation, and Scheduling in MIMO and OFDM Systems.* New York, NY, USA: Cambridge Univ. Press, 2011.

[20] A. Mengali, B. Shankar Mysore R. and B. Ottersten, "Exploring different receiver structures for radio over fso systems with signal dependent noise," in *Proc. IEEE Global Commun. Conf.*, 2017, pp. 1–7.